Published in final edited form as:
Biomaterials. 2011 May ; 32(13): 3387–3394. doi:10.1016/j.biomaterials.2011.01.025.

Mechanical properties and in vivo behavior of a biodegradable synthetic polymer microfiber - extracellular matrix hydrogel biohybrid scaffold

Yi Hong[1,2], **Alexander Huber**[1,2], **Keisuke Takanari**[1,2], **Nicholas J. Amoroso**[1,3], **Ryotaro Hashizume**[1,2], **Stephen F. Badylak**[1,2,3], and **William R. Wagner**[1,2,3,4,*]

[1]McGowan Institute for Regenerative Medicine, University of Pittsburgh, Pittsburgh, PA 15219, USA

[2]Department of Surgery, University of Pittsburgh, Pittsburgh, PA 15219, USA

[3]Department of Bioengineering, University of Pittsburgh, Pittsburgh, PA 15219, USA

[4]Department of Chemical Engineering, University of Pittsburgh, Pittsburgh, PA 15219, USA

Abstract

A biohybrid composite consisting of extracellular matrix (ECM) gel from porcine dermal tissue and biodegradable elastomeric fibers was generated and evaluated for soft tissue applications. ECM gel possesses attractive biocompatibility and bioactivity with weak mechanical properties and rapid degradation, while electrospun biodegradable poly(ester urethane)urea (PEUU) has good mechanical properties but limited cellular infiltration and tissue integration. A concurrent gel electrospray/polymer electrospinning method was employed to create ECM gel/PEUU fiber composites with attractive mechanical properties, including high flexibility and strength. Electron microscopy revealed a structure of interconnected fibrous layers embedded in ECM gel. Tensile mechanical properties could be tuned by altering the PEUU/ECM weight ratio. Scaffold tensile strengths for PEUU/ECM ratios of 67/33, 72/28 and 80/20 ranged from 80–187 kPa in the longitudinal axis (parallel to the collecting mandrel axis) and 41–91 kPa in the circumferential axis with 645–938% breaking strains. The 72/28 biohybrid composite and a control scaffold generated from electrospun PEUU alone were implanted into Lewis rats, replacing a full-thickness abdominal wall defect. At 4 wk, no infection or herniation was found at the implant site. Histological staining showed extensive cellular infiltration into the biohybrid scaffold with the newly developed tissue well integrated with the native periphery, while minimal cellular ingress into the electrospun PEUU scaffold was observed. Mechanical testing of explanted constructs showed evidence of substantial remodeling, with composite scaffolds adopting properties more comparable to the native abdominal wall. The described elastic biohybrid material imparts features of ECM gel bioactivity with PEUU strength and handling to provide a promising composite biomaterial for soft tissue repair and replacement.

Keywords

electrospinning; electrospray; polyurethane; extracellular matrix; hydrogel

*Corresponding author: William R. Wagner, wagnerwr@upmc.edu, Phone: 001-412-624-5324, Fax: 001-412-624-5363.

Introduction

Tissue-derived, extracellular matrix (ECM) materials have been shown to promote the site-specific, constructive remodeling of injured tissues and have been commonly used as surgical mesh devices in numerous preclinical and clinical trials [1]. The structural and biochemical complexity of ECM, i.e. its soluble and insoluble components [2], along with its spatial and temporal degradation at the site of repair, are critically important in the induction of desirable healing outcomes associated with these materials. In vivo, ECM materials elicit a controlled host tissue response through the recruitment of immunomodulatory cells of the innate immune system as well as stem and progenitor cells [3, 4], ultimately leading to positive, constructive tissue remodeling and regeneration.

A limitation of ECM-derived materials concomitant with their derivation from animal tissue sources and required processing is the limited range of mechanical properties that can be achieved and novel architectures that can be created. Relative to commonly applied biomedical polymers and metals, ECM materials cannot fulfill the mechanical needs of many medical device applications, thus ultimately preventing application of their biofunctionality in many settings. Post-production material processing techniques, such as chemical crosslinking, aimed at increasing ECM mechanical strength have been shown to also markedly alter constructive remodeling potential, resulting in a chronic, pro-inflammatory host response and the formation of fibrous scar tissue [5, 6].

Our objective in this study was to generate a biohybrid composite combining ECM with a synthetic biodegradable elastomer to create a material with improved bioactivity in vivo, in concert with mechanical properties not achievable with current ECM materials. While there have been previous reports of blends formed between ECM and synthetic polymers[7, 8], these blends compromise the mechanical properties of the polymer, and the solvent processing utilized may adversely impact the ECM bioactivity. To avoid this problem, we utilized a concurrent electrohydrodynamic processing approach where an elastomer was electrospun while an ECM gel was electrosprayed onto a rotating and rastering metallic collection mandrel (Figure 1A). Poly(ester urethane)urea (PEUU) was selected for the polymeric microfiber component because of its attractive elastomeric properties combined with a biodegradation profile in vivo of several months. This material has previously been utilized in vivo for a variety of cardiovascular [9–11], and abdominal wall applications [12]. A dermal ECM (dECM) hydrogel extracted from decellularized adult porcine dermis was selected for combination with PEUU due to its demonstrated chemoattractant capability [13]. The dECM solution prepared at neutral pH is fluid and capable of flowing freely between 4 and 25°C, becoming a solid hydrogel at 37°C. This thermal gelling behavior provided an opportunity to concurrently electrospin PEUU and electrospray dECM solution onto the same target to form a cohesive biohybrid construct, followed by warming to induce ECM gelation. The resultant biohybrid material was characterized in terms of its micro and macro morphology, uni- and bi-axial tensile properties, suture retention strength, and acute in vivo remodeling from both mechanical and histological perspectives. The effect of altering the polymer to ECM mass ratio was also explored within a defined range appropriate for soft tissue reconstructive procedures.

Materials and Methods

Dermal ECM solution preparation

Porcine skin was obtained from a local abattoir immediately after the death of pigs weighing approximately 100–120 kg. Connective tissue and epithelium were removed and the remaining tissue was placed in deionized water at 4°C for 24 h. The tissue was then placed

in 0.02% trypsin/0.05% ethylenediaminetetraacetic acid (EDTA) at 37°C for 5 h, and then placed on a rocker in 3% (v/v) Triton-X at 4°C for 48 h, then in 4% (w/v) deoxycholic acid at 4°C for 48 h. Dermal matrix was then treated with 0.1% peracetic acid/4% ethanol for 2 h at room temperature with rocking, and finally rinsed sequentially with phosphate buffer solution (PBS, 15 min), deionized water (15 min, 2x), and then PBS (15 min). The resulting dermal matrix sheets were rinsed in deionized water and lyophilized. Lyophilized sheets were comminuted into particulate form using a Waring commercial blender and Wiley Mill.

To digest the dermal matrix, particulate lyophilized matrix was added to 1 mg/mL pepsin in 0.01 N HCl for a final concentration of 20 mg matrix/mL suspension. The suspension was mixed on a stir plate at room temperature for 48 h, at which time no visible pieces of dermal matrix remained. To prepare 1 mL of a 10 mg/mL gel, 0.5 mL ECM digest, 0.11 mL 10X PBS, 0.1 mL 0.1N NaOH, and 0.29 mL 1X PBS were chilled and mixed together and used immediately for electrospraying. To verify that this pre-gel solution could form a gel, it was placed in a 37°C incubator and after approximately 2 h gel formation occurred.

Fabrication of PEUU/dECM hydrogel biohybrid scaffold

PEUU was synthesized as previously described from polycaprolactone diol (PCL, Mn=2000, Sigma) and 1,4-diisocynatobutane (BDI, Sigma) with putrescine (Sigma) as a chain extender at a 1:2:1 molar ratio [14]. A concurrent electrospin/electrospray method was used to fabricate the PEUU microfibers/dECM gel biohybrid composite scaffold (Figure 1A). Briefly, 10 mL of 10 mg/mL dECM solution at 4°C was fed by a syringe pump into a sterilized capillary (1.2 mm I.D.) charged at 7 kV and suspended 4 cm above the target stainless steel mandrel (19 mm diameter). Concurrently, PEUU in hexafluoroisopropanol (HFIP, Oakwood Products, United States) solution (12%, w/v) was fed at 20 mL/h from a capillary charged at 10 kV and perpendicularly located 20 cm from the target mandrel. The mandrel was charged at −4 kV and rotated at 250 rpm while translating back and forth 8 cm along its rotational axis at 0.15 cm/s. The biohybrid materials of different PEUU fiber to dECM ratios (80/20, 72/28, 67/33) were generated by different dECM solution infusion rates at 1, 1.5 and 2 mL/min, respectively. Biohybrid scaffolds were transferred from the mandrel (Figure 1B) to a Petri dish (Figure 1C) and left to gel up to 2 h at 37°C to allow complete dECM gelling (Figure 1D). An electrospun PEUU sheet without hydrogel electrospraying was fabricated as a control material.

Scaffold characterization

The scaffold surface and cross-sectional morphology were observed under scanning electron microscopy. The scaffold was frozen and broken in liquid nitrogen, lyophilized, and gold sputter-coated. The cross-sectional morphology of a biohybrid scaffold with a PEUU/dECM 72/28 wt% ratio was also observed using Masson's trichrome staining after formaldehyde fixation, paraffin embedding and sectioning.

A 2.5×20 mm strip cut from a biohybrid scaffold was used to measure uniaxial tensile strength and strain under a MTS Tytron 250 MicroForce Testing Workstation at a 2.5 cm/min crosshead speed, according to ASTM D638-98 (n=5). Suture retention strength was measured using a BIOSYN UM-214 4-0 suture under the same conditions. A single suture loop was created 5 mm from the short edge of a 5×20 mm strip and fixed on the upper clamp. Suture retention strength was calculated as suture load/(suture diameter × sample thickness) at the tearing point.

In vivo full-thickness abdominal wall replacement

A full thickness abdominal wall reconstruction was performed on adult female syngeneic Lewis rats (200–250 g). All animal related procedures were performed as approved by the

Institutional Animal Care and Use Committee of the University of Pittsburgh. Research was conducted in compliance with the Animal Welfare Act Regulations and other US statutes relating to animals and experiments involving animals and adheres to the principles set forth in the Guide for Care and Use of Laboratory Animals, National Research Council, 1996. The surgical procedure was based on methods previously reported by Lai et al [15] and recently described in Hashizume et al [12]. Briefly, a 3.5 cm incision was made 2 cm caudally of the xiphoid process in the midline of the abdomen and a rectangular defect (1×2.5 cm) involving the fascia, rectus abdominis muscle and peritoneum (with the exception of the skin and subcutaneous tissue) was created. This defect was reconstructed randomly with either PEUU/dECM 72/28 patches (n=7) or electrospun PEUU patches (n=7). The patches were sutured to residual muscle by a continuous suture without overlap between muscles and patches, in direct contact with subcutaneous tissue and peritoneal viscera. The skin was closed over the patch with a double layer suture. Animals were administered 0.1 mg/kg subcutaneous buprenorphine postoperatively as an analgesic twice/day for 3 days. The implanted scaffolds were recovered at 4 wks with representative specimens photographed in situ. The scaffolds were removed with the surrounding muscle by cutting along an apron border approximately 5 mm from the original suture line. The explanted abdominal wall thickness was measured using a caliper. Bi-axial mechanical properties were measured in all samples with historical data using the same procedure utilized for native tissue [12]. Masson's trichrome and immuno-staining for alpha-smooth muscle actin (SMA) and CD-68 were performed on explanted samples. SMA was stained using a mouse monoclonal antibody against alpha-smooth muscle actin (1:200, Abcam). CD68 was stained by a mouse anti-rat monoclonal antibody to CD68 (1:100, AbD Serotec). Nuclei were stained with 4′,6-diamidino-2-phenylindole (DAPI, 1:10,000, Sigma).

Biaxial mechanical testing

Biaxial mechanical testing was performed for patches prior to implantation and explantation using previously described methods [12]. A 10×10 mm piece was cut from each retrieved sample (not including the suture line). These sections were immersed into Ringer's solution supplemented with verapamil (0.5 mM) and ethylene glycol tetraacetic acid (EGTA, 0.5 mM) for 1 h prior to testing to obtain complete muscle fiber relaxation. Following pretreatment, samples were tested using a Lagrangian membrane tension (T, force/unit length) controlled protocol designed to apply equal biaxial tension to each sample up to a maximum of 200 N/m, or the largest tension that the material was capable of withstanding. 200 N/m was chosen as an upper limit for applied force based on previous work [12] demonstrating that this was the maximum tension that native tissue could reliably withstand without incurring damage. Samples were tested in a physiological saline bath at room temperature. Four thin slices of polypropylene suture (Ethicon) were affixed to the central region of each sample in order to track local tissue strains and compute the deformation gradient tensor F. Axial stresses were determined from F, defined as F11=CD and F22=LD (CD=circumferential direction, LD=longitudinal direction). Two loading protocols containing 10 cycles each were performed, the first was used to precondition the sample. Data were collected from the final cycle of the second protocol.

Statistical analysis

All results are presented as mean ± standard deviation unless mentioned otherwise. Statistical analysis for mechanical properties was performed using one-way ANOVA with Newman post hoc testing. Differences were considered significant below $\alpha=0.05$.

Results

Scaffold characterization

The formed biohybrid constructs appeared opaque white in color with a glistening surface (Figure 1D). Macroscopically, the material behaved as a single cohesive layer that was firm to the touch, yet highly flexible and elastic (Video 1, supplemental material). Scanning electron microscopy (SEM) revealed a surface of micron-scale fibers partially spanned by ECM gel (Figure 2A). Cross-sectional images of the constructs at different PEUU/dECM ratios demonstrated integrated regions that were enriched in PEUU fibers or in ECM gel (Figure 2B–2D). Examination of the cross-section at higher resolution further demonstrated the formation of a distinct lamellar structure (PEUU fiber-rich and ECM-rich) with inter-connecting fibers in the ECM-rich regions (Figure 2E). No gross differences were apparent in the cross-sectional morphology as the PEUU/dECM ratio was altered. Based on these imaging observations, a simplified model of the scaffold microstructure is shown in Figure 2F where microfiber rich layers are connected by ECM-rich layers containing fibers at lower density. Imaging of the PEUU/dECM 72/28 scaffold with Masson's trichrome staining, where collagen appears blue, is shown in Figure 3. The blue staining further accentuates the lamellar structure of the blue ECM-rich and the white PEUU-rich regions.

Uni-axial mechanical properties

The tensile properties of the constructs were tunable by altering the PEUU/dECM mass ratios, accomplished by manipulating the flow rate of the dECM electrospray solution. Uniaxial tensile strength increased with increasing PEUU wt%, ranging from 80–187 kPa in the longitudinal axis (parallel to the collecting mandrel axis) and 41–91 kPa in the circumferential axis (Figure 4A). Peak strains were demonstrated to be over 600% for all scaffolds (Figure 4B). Suture retention strength ranged from 7–9 MPa (Figure 4C, Video 2, supplemental material), roughly comparable to the 23 MPa strength of expanded poly(tetrafluoroethylene) used clinically [16].

In vivo abdominal wall placement

Biohybrid scaffolds with a 72/28 PEUU/dECM wt% ratio were implanted into a rat full-thickness defect abdominal wall model to evaluate the potential for cellular infiltration and scaffold remodeling. Following the 4 wk implantation period no herniation, tissue adhesion, or infection were observed at the surgical sites for either the control electrospun PEUU or the biohybrid PEUU/dECM scaffold (Figure 5). The control electrospun PEUU scaffold without dECM and its periphery was apparent at the surgical site (Figure 5A), however for the biohybrid scaffold the material border was not clear (Figure 5B). The thickness of the explant site for the biohybrid construct (1.10 ± 0.16 cm) was similar to that of the native abdominal wall (0.97 ± 0.18 cm) and the electrospun PEUU (0.86 ± 0.06 cm) ($p > 0.05$). Minimal cellular infiltration was found for the electrospun PEUU scaffolds as was evident from the Masson's trichrome stained explanted cross-sections (Figure 6A and 6C). In contrast, cross-sections of the biohybrid scaffold demonstrated extensive cellular infiltration (Figure 6B and 6D). Immunofluorescence microscopy also revealed minimal cellular infiltration for the electrospun PEUU scaffold (Figure 6E), but extensive ingress of macrophages (CD68 positive cells) and smooth muscle actin expressing cells for the biohybrid scaffold (Figure 6F).

Biaxial mechanical properties

Under planar biaxial mechanical loading, we observed softer behavior of the 72/28 PEUU/dECM wt% material prior to implantation (Figure 7A and 7B) relative to the native abdominal wall tissue. The latter showed markedly anisotropic behavior with greater

stiffness in the circumferential direction of the rat. After the 4 wk implantation period, biaxial mechanical testing of explanted biohybrid constructs showed a marked change in tensile properties with an increase in stiffness towards values comparable to native tissue and a display of similar anisotropy. (Figure 7A and 7B)

Discussion

The electrospinning process has been widely investigated as a method to form fibrous scaffold materials with individual fibers at the micron and submicron size scale, having some structural similarity to the ECM. A wide variety of synthetic materials have been electrospun to create scaffolds for application in a variety of tissue settings including bone, cartilage, ligament, tendon, skin, nerves, and blood vessels [17, 18]. However, the dense fibrous structure characteristic of the electrospinning process most commonly hampers cellular infiltration, creating a major limitation in the generation of three-dimensional tissue constructs in vitro or in vivo, and ultimately limiting clinical applicability. Several modified processes have been developed to address this limitation including ice crystal deposition [19] and electrospraying of salt particles [20], hydrogels [21], cell culture medium [12] and cell suspensions [22]. Among these, a concurrent electrospun fiber, electrosprayed hyaluronic acid-derivative gel method reported by Ekaputra et al. has similarities to the current study, although mechanical properties and the in vivo response were not reported [21]. The hydrogel in that study was a commercial hydrogel, Heprasil, based on chemically modified hyaluronic acid and heparin that was electrosprayed after mixing with a chemical crosslinking agent, but before the initiated crosslinking led to gelation. The resulting materials showed better fetal osteoblast penetration in vitro compared to electrospun fibers alone.

Hydrogels derived from digested ECMs have theoretical advantages over gels isolated from purified individual ECM components and several such gels have recently been characterized and applied in a number of settings. For instance, urinary bladder matrix derived gel has been associated with better smooth muscle cell growth than type I collagen gels [23]. Human hepatocyte function has been shown to be maintained in a liver-derived ECM gel [24]. Small intestinal submucosa (SIS) gel preserved end-systolic left ventricular geometry and improved cardiac contractility when it was injected into ischemic myocardium in a murine rat model of an acute myocardial infarction [25]. ECM digest from dermal tissue, similar to that used in this study, has been shown to contain numerous peptides in the 15 – 250 kDa range with in vitro chemoattractant activity for human keratinocyte progenitor and stem cells [13].

We reported here the use of a two-nozzle system where a dermal ECM gel was deposited independently of the polymeric fibers. Previous reports have created blended material in the organic solvent HFIP and then electrospun the mixture into a fibrous composite scaffold [7, 8]. The direct contact of organic solvent with ECM proteins might result in the partial loss of bioactivity. For example, a main component in ECM, collagen, has been shown by investigators to lose varying degrees of tertiary structure under HFIP processing [7, 26, 27]. By separating the ECM gel solution into a separate delivery path, exposure to the highly volatile organic component is minimized and, although not examined in this study, would be expected to sustain relatively higher levels of bioactivity.

Several limitations in this study should be noted. First, for the in vivo evaluation, an extended study would be justified to follow the complete remodeling process of the material. Our objective here was to examine the acute response and demonstrate rapid cellular infiltration, which was clearly evident at the 4 week time point. Extended implant periods would be necessary to investigate the potential maturation of the healing response from a

macrophage-dominated cellular response, to a potentially more functional tissue, such as the development of site-appropriate skeletal muscle bundles. Second, although infiltrating macrophages defined by CD68 expression were demonstrated, it would be of interest to further characterize macrophage phenotype in terms of M1 (pro-inflammatory) or M2 (constructive remodeling) markers [6, 28]. Tracking the spatial and temporal patterns of M1 and M2 macrophages could yield insight into the remodeling process for this composite material. One might expect more inflammatory behavior to be associated with the degrading synthetic polymer components and more constructive remodeling in the ECM gel regions.

The described processing approach provides opportunities to develop bioactive scaffolds with tunable characteristics for tissue repair and replacement. The technique is not limited to the polymer and hydrogel used in this report. The dECM gel could be combined with polymers having different mechanical profiles (e.g. stiffer) and with non-degradable fibers that would permanently reside in vivo following ECM remodeling. Other ECM digest sources could also be evaluated in this system. ECM gels from SIS, urinary bladder and liver have been described, and given the variability in non-digested ECM behavior, it is reasonable to expect different bioactivity on the part of the derivative gels [23–25]. Choosing appropriate polymer and hydrogel combinations would allow the design of biohybrid scaffolds to meet the tissue reconstruction needs in a variety of settings, such as cardiovascular, pelvic floor, skin and nervous tissue.

Conclusions

A biohybrid scaffold material has been generated with a complex lamellar structure containing elastic, biodegradable polymer microfibers interspersed with ECM hydrogel by employing a concurrent electrospin/electrospray method. Such scaffolds were shown to possess attractive mechanical properties with high flexibility and soft tissue-like behavior. In vivo the biohybrid material facilitated a high degree of cellular infiltration relative to purely synthetic analogue material, and also was mechanically remodeled to better approximate native abdominal wall tissue. This biohybrid composite approach offers a method to overcome a major limitation associated with ECM-based materials by broadening the range of mechanical properties that can be achieved by ECM materials or ECM gels alone.

Supplementary Material

Refer to Web version on PubMed Central for supplementary material.

Acknowledgments

This work was supported in part by the Armed Forces Institute for Regenerative Medicine (AFIRM, #W81XWH-08-2-0032) and NIH R01 HL-068816. We also thank Prof. Michael S. Sacks for use of the biaxial mechanical testing device and Deanna Rhoads for histological sectioning.

References

1. Cornwell KG, Landsman A, James KS. Extracellular matrix biomaterials for soft tissue repair. Clin Podiatr Med Surg. 2009; 26:507–23. [PubMed: 19778685]
2. Badylak SF, Freytes DO, Gilbert TW. Extracellular matrix as a biological scaffold material: Structure and function. Acta Biomater. 2009; 5:1–13. [PubMed: 18938117]
3. Vorotnikova E, McIntosh D, Dewilde A, Zhang J, Reing JE, Zhang L, et al. Extracellular matrix-derived products modulate endothelial and progenitor cell migration and proliferation in vitro and stimulate regenerative healing in vivo. Matrix Biol. 2010; 29:690–700. [PubMed: 20797438]

4. Tottey S, Corselli M, Jeffries EM, Londono R, Peault B, Badylak SF. Extracellular matrix degradation products and low-oxygen conditions enhance the regenerative potential of perivascular stem cells. Tissue Eng Part A. 2011; 17:37–44. [PubMed: 20653348]
5. Valentin JE, Stewart-Akers AM, Gilbert TW, Badylak SF. Macrophage participation in the degradation and remodeling of extracellular matrix scaffolds. Tissue Eng Part A. 2009; 15:1687–94. [PubMed: 19125644]
6. Badylak SF, Valentin JE, Ravindra AK, McCabe GP, Stewart-Akers AM. Macrophage phenotype as a determinant of biologic scaffold remodeling. Tissue Eng Part A. 2008; 14:1835–42. [PubMed: 18950271]
7. Stankus JJ, Freytes DO, Badylak SF, Wagner WR. Hybrid nanofibrous scaffolds from electrospinning of a synthetic biodegradable elastomer and urinary bladder matrix. J Biomater Sci Polym Ed. 2008; 19:635–52. [PubMed: 18419942]
8. Yoon H, Kim G. Micro/nanofibrous scaffolds electrospun from PCL and small intestinal submucosa. J Biomater Sci Polym Ed. 2010; 21:553–62. [PubMed: 20338091]
9. Fujimoto KL, Tobita K, Merryman WD, Guan J, Momoi N, Stolz DB, et al. An elastic, biodegradable cardiac patch induces contractile smooth muscle and improves cardiac remodeling and function in subacute myocardial infarction. J Am Coll Cardiol. 2007; 49:2292–300. [PubMed: 17560295]
10. Hong Y, Ye SH, Nieponice A, Soletti L, Vorp DA, Wagner WR. A small diameter, fibrous vascular conduit generated from a poly(ester urethane)urea and phospholipid polymer blend. Biomaterials. 2009; 30:2457–67. [PubMed: 19181378]
11. He W, Nieponice A, Soletti L, Hong Y, Gharaibeh B, Crisan M, et al. Pericyte-based human tissue engineered vascular grafts. Biomaterials. 2010; 31:8235–44. [PubMed: 20684982]
12. Hashizume R, Fujimoto KL, Hong Y, Amoroso NJ, Tobita K, Miki T, et al. Morphological and mechanical characteristics of the reconstructed rat abdominal wall following use of a wet electrospun biodegradable polyurethane elastomer scaffold. Biomaterials. 2010; 31:3253–65. [PubMed: 20138661]
13. Brennan EP, Tang XH, Stewart-Akers AM, Gudas LJ, Badylak SF. Chemoattractant activity of degradation products of fetal and adult skin extracellular matrix for keratinocyte progenitor cells. J Tissue Eng Regen Med. 2008; 2:491–8. [PubMed: 18956412]
14. Guan J, Sacks MS, Beckman EJ, Wagner WR. Synthesis, characterization, and cytocompatibility of elastomeric, biodegradable poly(ester-urethane)ureas based on poly(caprolactone) and putrescine. J Biomed Mater Res. 2002; 61:493–503. [PubMed: 12115475]
15. Lai PH, Chang Y, Liang HC, Chen SC, Wei HJ, Sung HW. Peritoneal regeneration induced by an acellular bovine pericardial patch in the repair of abdominal wall defects. J Surg Res. 2005; 127:85–92. [PubMed: 15921700]
16. Hong Y, Fujimoto K, Hashizume R, Guan J, Stankus JJ, Tobita K, et al. Generating elastic, biodegradable polyurethane/poly(lactide-co-glycolide) fibrous sheets with controlled antibiotic release via two-stream electrospinning. Biomacromolecules. 2008; 9:1200–7. [PubMed: 18318501]
17. Kumbar SG, James R, Nukavarapu SP, Laurencin CT. Electrospun nanofiber scaffolds: engineering soft tissues. Biomed Mater. 2008; 3:034002. [PubMed: 18689924]
18. Jang JH, Castano O, Kim HW. Electrospun materials as potential platforms for bone tissue engineering. Adv Drug Deliv Rev. 2009; 61:1065–83. [PubMed: 19646493]
19. Leong MF, Rasheed MZ, Lim TC, Chian KS. In vitro cell infiltration and in vivo cell infiltration and vascularization in a fibrous, highly porous poly(D, L-lactide) scaffold fabricated by cryogenic electrospinning technique. J Biomed Mater Res A. 2009; 91:231–40. [PubMed: 18814222]
20. Nam J, Huang Y, Agarwal S, Lannutti J. Improved cellular infiltration in electrospun fiber via engineered porosity. Tissue Eng. 2007; 13:2249–57. [PubMed: 17536926]
21. Ekaputra AK, Prestwich GD, Cool SM, Hutmacher DW. Combining electrospun scaffolds with electrosprayed hydrogels leads to three-dimensional cellularization of hybrid constructs. Biomacromolecules. 2008; 9:2097–103. [PubMed: 18646822]

22. Stankus JJ, Soletti L, Fujimoto K, Hong Y, Vorp DA, Wagner WR. Fabrication of cell microintegrated blood vessel constructs through electrohydrodynamic atomization. Biomaterials. 2007; 28:2738–46. [PubMed: 17337048]

23. Freytes DO, Martin J, Velankar SS, Lee AS, Badylak SF. Preparation and rheological characterization of a gel form of the porcine urinary bladder matrix. Biomaterials. 2008; 29:1630–7. [PubMed: 18201760]

24. Sellaro TL, Ranade A, Faulk DM, McCabe GP, Dorko K, Badylak SF, et al. Maintenance of human hepatocyte function in vitro by liver-derived extracellular matrix gels. Tissue Eng Part A. 2010; 16:1075–82. [PubMed: 19845461]

25. Okada M, Payne TR, Oshima H, Momoi N, Tobita K, Huard J. Differential efficacy of gels derived from small intestinal submucosa as an injectable biomaterial for myocardial infarct repair. Biomaterials. 2010; 31:7678–83. [PubMed: 20674011]

26. Zeugolis DI, Khew ST, Yew ES, Ekaputra AK, Tong YW, Yung LY, et al. Electro-spinning of pure collagen nano-fibres - just an expensive way to make gelatin? Biomaterials. 2008; 29:2293–305. [PubMed: 18313748]

27. Matthews JA, Wnek GE, Simpson DG, Bowlin GL. Electrospinning of collagen nanofibers. Biomacromolecules. 2002; 3:232–8. [PubMed: 11888306]

28. Brown BN, Valentin JE, Stewart-Akers AM, McCabe GP, Badylak SF. Macrophage phenotype and remodeling outcomes in response to biologic scaffolds with and without a cellular component. Biomaterials. 2009; 30:1482–91. [PubMed: 19121538]

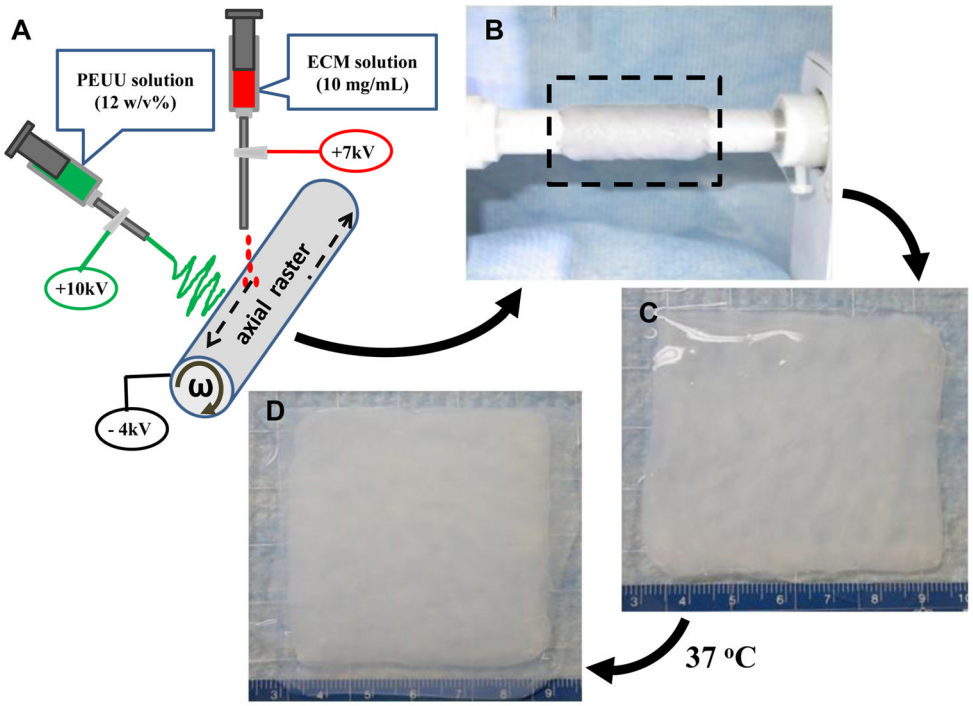

Figure 1.

Concurrent electrospin/electrospray technique for PEUU/dECM biohybrid scaffold fabrication (**A**). After processing (**B**), the biohybrid sheet containing PEUU microfibers and ECM hydrogel solution (**C**) was removed from the mandrel and heated to 37°C. After 2 h, the PEUU/dECM hydrogel hybrid scaffold was formed (**D**).

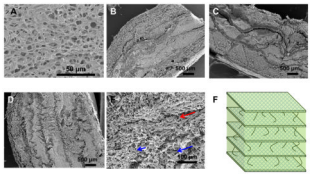

Figure 2.
Electron micrographs of biohybrid scaffold surfaces showed PEUU fibers spanned by dECM gel (**A**). The cross-sections of 80/20 (**B**), 72/28 (**C**) and 67/33 (**D**) PEUU/dECM wt% scaffolds were lamellar with regions rich in PEUU fibers and regions of dECM gel with fewer fibers. A magnified region from the 80/20 scaffold illustrates the presence of a PEUU fiber-rich lamella and less dense connecting fibers interspersed in the dECM material (red arrow points to fiber-rich region and blue arrows point to sparse fibers) (**E**). A simplified representation of the biohybrid scaffold architecture with lamellae enriched with PEUU fibers separated by dECM rich regions with interconnecting fibers (**F**).

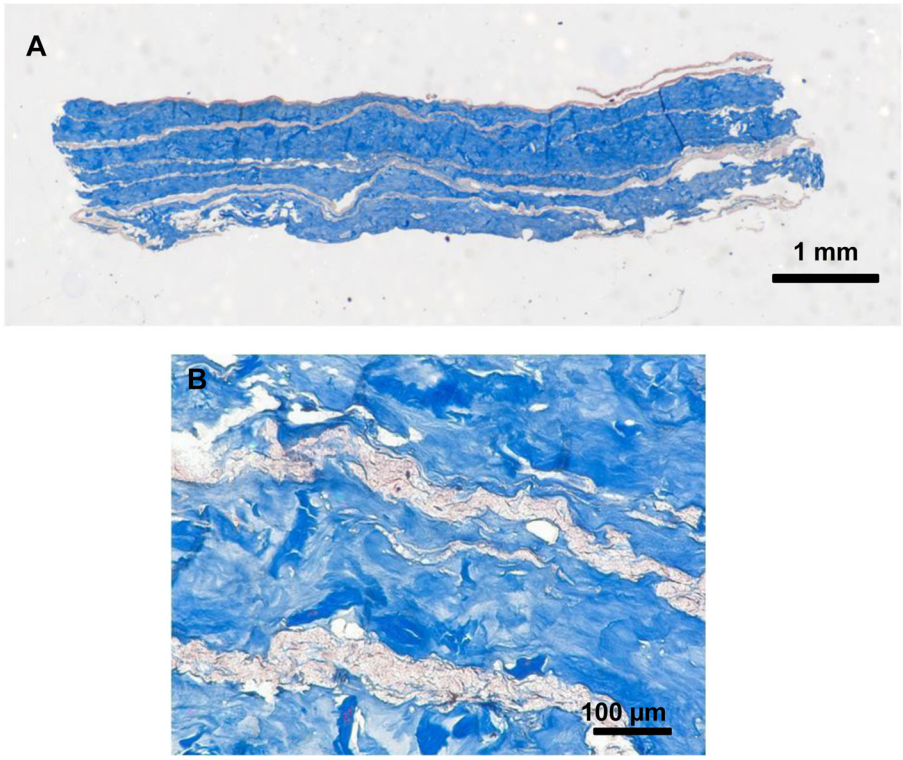

Figure 3.
Masson's trichrome staining of the cross-section of the PEUU/dECM 72/28 biohybrid scaffold emphasizes the alternating microfiber and hydrogel rich regions with a full-view (**A**) and a magnified (**B**) image.

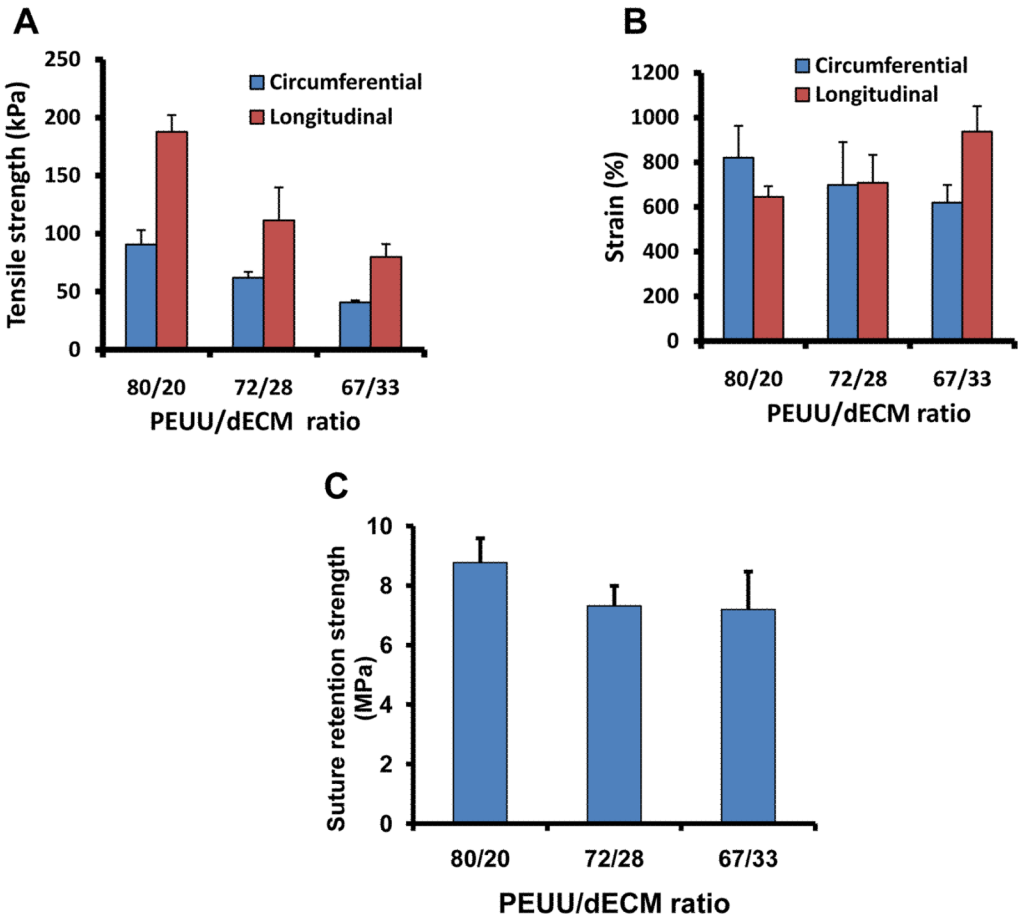

Figure 4.

By altering the PEUU/dECM mass ratio the scaffold peak tensile strength could be tuned in the circumferential axis (**A**), whereas the effect on peak strain was not as apparent (**B**). The suture retention strength was relatively high for all samples. At the highest PEUU content a slight, but significantly greater strength was measured (**C**).

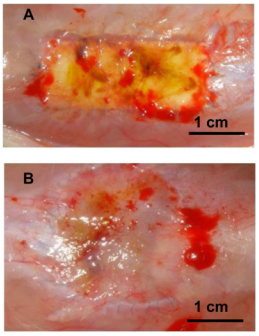

Figure 5.
The control electrospun PEUU scaffold (**A**) and the biohybrid PEUU/dECM 72/28 scaffold (**B**) are seen at the time of explant from the abdominal wall defect after 4 wk.

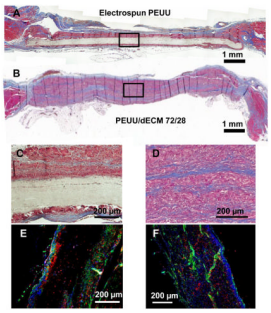

Figure 6.

Masson's trichrome stained explanted cross-sections showed minimal cellular infiltration in the electrospun PEUU (**A**), and extensive cellular infiltration into the biohybrid scaffold (**B**). A magnified image of electrospun PEUU showed minimal cellular ingress with tissue encapsulation (**C**). A magnified image emphasizes the cellularity and extracellular matrix deposition, as well as remnant polymer fibers (white) for the biohybrid scaffold (**D**). Immunohistochemistry of the electrospun scaffold shows surrounding macrophage (red, CD68) and positive smooth muscle actin expression(green) (**E**), however Immunohistochemistry of the biohybrid explanted material shows macrophage infiltration (red, CD68) and positive smooth muscle actin expression (green) (**F**).

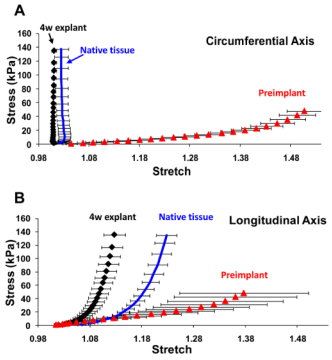

Figure 7.

Biaxial mechanical testing of scaffolds prior to implant and after 4 wk in situ for the PEUU/dECM 72/28 scaffold are presented in (**A**) for the circumferential axis and (**B**) for the longitudinal axis. Native rat abdominal wall tissue behavior is also presented, from ref. 12. The mechanical remodeling towards native tissue behavior is apparent.